Multidimensional short-pulse space-charge-limited flow

W. S. Koh
School of Electrical and Electronic Engineering, Nanyang Technological University, Singapore 639798

L. K. Ang[a)]
School of Electrical and Electronic Engineering, Nanyang Technological University, Singapore 639798 and Institute of High Performance Computing, Singapore 117528

T. J. T. Kwan
Applied Physics Division, Los Alamos National Laboratory, Los Alamos, New Mexico 87545

(Received 24 March 2006; accepted 4 May 2006; published online 12 June 2006)

The two-dimensional models of the space-charge-limited (SCL) current density at the short pulse limit for which the electron pulse length is comparable or smaller than the electron transit time across the gap (i.e., $X_{\mathrm{CL}} \leqslant 1$) have been developed. In particular, the scaling laws for short-pulse SCL electron emission in a planar diode with a circular emitting strip and a cylindrical diode with a finite length have been obtained and verified with particle-in-cell simulation. It is found that the enhancement (in terms of the long-pulse SCL current density) is proportional to X_{CL}^{-1} for small X_{CL} for both planar and cylindrical cases. The enhancement of the cylindrical short-pulse SCL current density is also found to be larger for the convergent flow (cathode outside) than divergent flow (cathode inside). Multidimensional effects are important only for small emitting strips with size comparable to the effective penetration distance (into the gap) of the short-pulse electron beam. Smooth transition between the short-pulse regime and the long pulse (steady-state) regime is demonstrated. © *2006 American Institute of Physics*. [DOI: 10.1063/1.2208086]

I. INTRODUCTION

Photocathode guns have shown to be an excellent electron source used in many free-electron lasers (FEL) facilities around the world.[1–4] Besides being able to emit high currents (>100 mA), low emittances and low energy spread of the electron beam from a photocathode are also critical in FEL. Electron emission from traditional photocathodes are normally source limited and the amount of emitted current or charges is limited by the quantum efficiency of the materials. Recently, photoinjectors using novel cathodes such as niobium photocathode,[5] carbon or ceramic-coated metal cathodes,[6] Cs ion-implanted metal cathodes,[7] Scandate dispenser cathodes,[8] and needle-like cathodes,[9] have shown improvements in its quantum efficiencies and robustness, in order to produce short bunches of electron beam with high charge density on the order of nC per bunch. Improvements in ultrafast laser technology[10,11] have also enabled photocathodes to operate in the space-charge-limited (SCL) regime generating very high charges (several nC) in each pulse.

The classical SCL electron emission gives the maximum steady-state (or long pulse) current density that can be transported across a vacuum gap of spacing D and potential difference V_g without virtual cathode formation. The one-dimensional (1D) SCL emission current density in a planar diode is the well-known Child-Langmuir (CL) law[12,13] given by

$$J_{\mathrm{CL}} = \frac{4}{9}\epsilon_o \sqrt{\frac{2e}{m_e}}\frac{V_g^{3/2}}{D^2}, \tag{1}$$

where e and m_e are the charge and mass of the electron respectively, and ϵ_0 is the free space permittivity. The equivalent SCL emission for a cylindrical diode is the Langmuir-Blodgett (LB) law[14] given by

$$J_{\mathrm{LB}} = \frac{8\pi}{9}\epsilon_0 \sqrt{\frac{2e}{m_e}}\frac{V_g^{3/2}}{r_a \beta_a^2}, \tag{2}$$

where r_a (and r_c) is the radius of the anode (and cathode), and $\beta_a = f(\gamma_a)$ is a series expansion of $\gamma_a = r_a/r_c$.[14] In the earlier works,[12–14] the traditional long pulse SCL emission has been studied quite intensively to include various effects, such as finite emission velocity,[15–18] relativistic model,[19] quantum models[20–22] and multidimensional models for both planar[23–26] and cylindrical[26,27] geometries.

For a short electron bunch of SCL emission, the pulse length of the electron beam (from photoinjector) is usually shorter than the transit time of the electrons across the gap. Thus, the classical scaling laws such as CL law and LB law, which were derived based on steady-state condition (or long pulse limit) are no longer valid for short pulse SCL emission like those emitted from high current photocathodes.[28–30] It has also been shown that the traditional long-pulse CL law can be enhanced by a large factor at the short-pulse limit in a recent experiment, and the 1D short-pulse CL law has been formulated and confirmed with particle-in-cell (PIC) simulation.[30]

Most of the photoinjectors in the major FEL facilities make use of the planar photocathodes for which the emission area may not be one-dimensional in nature, especially if novel needle-like field emitters are used. The finite dimensions and shape of the photocathodes may further raise the limit of the SCL current density, which is analogous to the multidimensional steady-state SCL models.[23,25,26] Dowell *et al.*[1] have also suggested that photocathodes may be an excellent electron source for vircators (usually in the cylindrical

[a)]Electronic mail: elkang@ntu.edu.sg

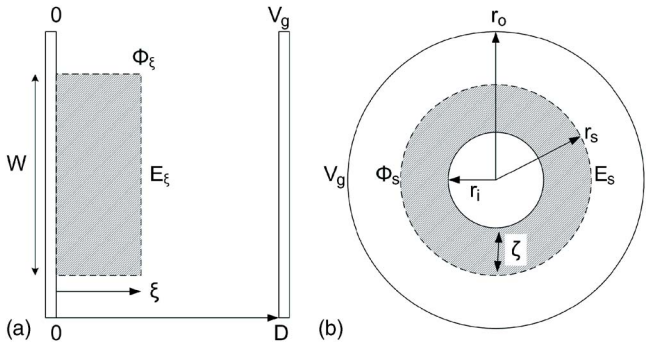

FIG. 1. (a) A 1D planar diode of gap spacing D with a short pulse propagating a distance $x=\xi$ into the vacuum gap having a potential of ϕ_ξ and electric field E_ξ at the interface of the electron pulse and vacuum. (b) A 1D cylindrical diode (cathode inside) of outer radius r_o and inner radius r_i with a short pulse of pulse length ζ propagating to a radial position $r=r_s$ of the vacuum gap having a potential of ϕ_s and electric field E_s at the interface of the electron pulse and vacuum. The cathode is grounded and a potential of V_g is applied at the anode.

configurations) as a short-pulse rf photoinjector beam, which is capable of oscillating spontaneously and has the potential to improve the microwave generation efficiency of these compact devices.

Thus, in this context, several questions arise: How does one derive a two-dimensional (2D) short-pulse CL law that is valid with finite emission area (like a circular patch of radius R)? What is the corresponding 1D and 2D short-pulse LB law for a cylindrical diode? Can the analytical scaling laws for of various 2D [or three-dimensional (3D)] emitting features formulated for the long-pulse SCL emission be readily applicable for the short-pulse SCL emission? This article will address these questions.

II. THEORY AND SIMULATIONS

A. 1D planar short-pulse CL law

Using the methodology proposed by Valfells *et al.*,[30] we will briefly review the formulation of the 1D short-pulse CL law. Consider an 1D planar diode of gap spacing D, with a grounded cathode, and a potential of V_g is applied to the anode. An uniform electron beam (of zero initial velocity and current density J) with a finite pulse length τ_p is injected normally into the vacuum gap from the cathode as shown in Fig. 1(a). As τ_p is shorter than the SCL electron transit time $T_{\mathrm{CL}}=3D/\sqrt{2eV_g/m_e}$, the electron beam can only extend to a distance of ξ, which is smaller than the gap spacing D. At the beam-vacuum interface of $x=\xi$, the potential and electric fields are, respectively, ϕ_ξ and E_ξ.

To obtain the SCL current density $J=J_{cp}(1\mathrm{D})$ at the short-pulse limit, we assume that the SCL emission occurs in an equivalent diode with a gap spacing of ξ having a potential difference of ϕ_ξ, and the related normalized 1D short pulse CL law is

$$\mu_{cp}(1\mathrm{D})=\frac{\bar{\phi}_\xi^{3/2}}{\bar{\xi}^2}, \tag{3}$$

where $\mu_{cp}(1\mathrm{D})=J_{cp}(1\mathrm{D})/J_{\mathrm{CL}}$, $\bar{\xi}=\xi/D$, and $\bar{\phi}_\xi=\phi_\xi/V_g$. Under this condition, the electric field at $x=\xi$ is continuous, which has the normalized form of $\bar{E}_\xi=E_\xi/(V_g/D)$:

$$\bar{E}_\xi=-\frac{4\bar{\phi}_\xi}{3\bar{\xi}}=-\frac{\bar{\phi}_\xi-1}{\bar{\xi}-1}. \tag{4}$$

By considering the electron beam as a single sheet of electrons with a charge density of $\sigma=J\tau_p$, the change in the electric field (due to space-charge effects) can be expressed as $E-E_c=-\sigma/\epsilon_0$, which becomes $E=-\sigma/\epsilon_0=J\tau_p/\epsilon_0$ when the electric field at the cathode E_c is driven to zero by the space-charge effect. Thus at $E=E_\xi$ and $J=J_{cp}(1\mathrm{D})$, we obtain a relationship between $\bar{\phi}_\xi$, $\bar{\xi}$, and the normalized transit time $(0\leqslant X_{\mathrm{CL}}=\tau_p/T_{\mathrm{CL}}\leqslant 1)$, which is given by

$$X_{\mathrm{CL}}\bar{\phi}_\xi^{1/2}=\bar{\xi}. \tag{5}$$

Thus, by solving Eqs. (3)–(5), the equations may be expressed as a function of X_{CL}, which are

$$\mu_{cp}(1\mathrm{D})=\frac{2}{X_{\mathrm{CL}}^3}\left(1-\sqrt{1-\frac{3}{4}X_{\mathrm{CL}}^2}\right), \tag{6a}$$

$$\bar{\phi}_\xi^{1/2}=\frac{2}{X_{\mathrm{CL}}}\left(1-\sqrt{1-\frac{3}{4}X_{\mathrm{CL}}^2}\right), \tag{6b}$$

$$\bar{\xi}=2\left(1-\sqrt{1-\frac{3}{4}X_{\mathrm{CL}}^2}\right). \tag{6c}$$

At $X_{\mathrm{CL}}=1$, we have $\mu_{cp(1\mathrm{D})}=1$, where the 1D short-pulse CL law recovers to the 1D classical long-pulse CL law as expected. At small $X_{\mathrm{CL}}\ll 1$, they are $\mu_{cp}(1\mathrm{D})=\frac{3}{4}X_{\mathrm{CL}}^{-1}$, $\bar{\phi}_\xi^{1/2}=\frac{3}{4}X_{\mathrm{CL}}$, and $\bar{\xi}=\frac{3}{4}X_{\mathrm{CL}}^2$. Note that the diode is simply a capacitor with total charge $Q=CV$ before any emission, and the total charge that can be liberated for short duration of SCL electron emission is always less than or equal to the induced surface charge.[30]

B. 1D cylindrical short-pulse CL law

Based on the equivalent diode model, we will derive the corresponding 1D short-pulse LB law for both convergent and divergent flows. Consider a cylindrical diode with a divergent electron flow extending from an inner cathode at $r=r_c=r_i$ to a outer anode at $r_a=r_o$. The cathode is grounded and a potential of V_g is applied at the anode. A uniform sheet of electrons (of zero emission energy and current density J) with a pulse length of τ_p (shorter than the electron transit time) extends from the cathode to a point $r=r_s$ inside the gap as illustrated in Fig. 1(b), where the potential and electric field at the beam-vacuum interface $(r=r_s)$ are denoted as ϕ_s and E_s, respectively. With a beam thickness of $\zeta=r_s-r_c<D$, the normalized 1D short-pulse LB law (in terms of its long-pulse limit) is

$$\chi_{cc(1D)} = \frac{\bar{\phi}_s}{\bar{r}_s \bar{\beta}_s^2}, \tag{7}$$

where $\chi_{cc(1D)} = J_{cc}(1D)/J_{LB}$, $\bar{\phi}_s = \phi_s/V_g$, $\bar{r}_s = r_s/r_a$, and $\bar{\beta}_s = \beta_s/\beta_a$. Here, $\beta_s = f(\gamma_s)$ and $\beta_a = f(\gamma_a)$ is, respectively, the series expansion of $\gamma_s = r_s/r_c$, and $\gamma_a = r_a/r_c$ from the 1D long-pulse LB law.[14]

To obtain the dependence of $\bar{\phi}_s$, and $\bar{r}_s$ as a function of the normalized transit time X_{CL}, we solve for the electric field at the beam front E_s as a function ϕ_s and r_s at the SCL condition. The contributions of the $d\bar{\phi}/d\bar{r}$ term in the cylindrical Poisson equation can be neglected as the electric field (in the region near to the cathode) approaches zero (i.e., $d\bar{\phi}/d\bar{r} \to 0$) at the SCL condition. In doing so, the normalized electric field $\bar{E}_s = E_s/[V_g/(r_a\beta_a)]$ is formulated as $\bar{E}_s = -\alpha\bar{\phi}_s/\bar{r}_s\beta_s$, where $\alpha = f(r_s) > 0$ is the gradient of the potential at $r = r_s$, which can be obtained by solving numerically the 1D Poisson equation of the equivalent cylindrical diode. By matching the electric field at the beam-vacuum interface (i.e., $r = r_s$), the normalized electric field, $\bar{E}_s$ becomes

$$\bar{E}_s = -\alpha\frac{\bar{\phi}_s}{\bar{r}_s\bar{\beta}_s} = -\frac{(\bar{\phi}_s - 1)\beta_a}{\bar{r}_s\, ln(\bar{r}_s)}, \tag{8}$$

which can be solved for $\bar{\phi}_s$, given by

$$\bar{\phi}_s = \frac{1}{1 - \frac{\alpha}{\beta_s} ln(\bar{r}_s)}. \tag{9}$$

For the single sheet model in the cylindrical configuration under the SCL condition [i.e., $E = E_s$ and $J = J_{cc}(1D)$], the corresponding relationships between ϕ_s, r_s and X_{CL} are

$$X_{CL}\bar{\phi}_s^{1/2} = \frac{3}{4}\alpha\frac{r_s}{D}\beta_s \tag{10}$$

where $D = r_o - r_i$. For convergent flow, where the outer shell and inner shell is the cathode and the anode ($r_c = r_o > r_a = r_i$) respectively, the formulation of Eqs. (7)–(10) remains valid. However, as the direction of the convergent flow is opposite to the divergent, the α parameter shown in Eq. (10) becomes $-\alpha$, where α is negative for the convergent flow.

At a given r_a and r_c, we solve Eqs. (9) and (10) for $\bar{\phi}_s$ and X_{CL} by using $\bar{r}_s$ as a free parameter, which will give the corresponding values of β_s and α. By substituting $\bar{r}_s$ and $\bar{\phi}_s$ into Eq. (7), we obtain the normalized 1D short-pulse LB Law (in terms of the steady-state LB law) as a function X_{CL}. At $r_s \approx r_c$, we have α approaches $\pm 4/3$, and β_s becomes ξ/r_s, which will recover to the 1D planar limit.

C. 2D models of short-pulse SCL electron emission

The enhancement of the steady-state SCL electron flows (in terms of the 1D model) due to finite emission area is of the form $1 + F \times G$, where F and G are, respectively, the correction factors for electron's mean position and geometry of the various types of emitting patches.[26] For simplicity, we will consider two types of emitting patches to study the 2D models for short-pulse CL and LB law formulated earlier.

For the 2D short-pulse CL law, we consider a circular emitting patch of radius R on a planar cathode (of spacing D), which has a geometrical correction factor of $G = 4/(R/D)$[26] based on long-pulse formulation. Assuming the G factor is also valid for the short-pulse equivalent diode of a beam thickness of ξ, the enhancement of the 2D short-pulse CL law over the 1D short pulse CL law shown in Eq. (6) is

$$\kappa_{cp} = 1 + \frac{4}{R/\xi} \times F = 1 + \frac{4}{R/D}\bar{\xi} \times F \tag{11}$$

where $F = 1/4$[26] for nonrelativistic electrons with zero emission energy and $\bar{\xi}$ is a function of X_{CL} [see Eq. (6c)].

For the 2D short-pulse LB law, we study a cylindrical cathode with a finite length W, which has an enhancement factor in the form of $1 + (4/\pi)/(W/D) \times F(\Gamma)$, where $D = r_o - r_i$ is the gap distance between the cathode and anode, and $\Gamma = r_o/r_i$ is the aspect ratio of the of the cylindrical diode.[26] Based on the same argument of equivalent diode, the normalized 2D short-pulse LB law (in terms of the 1D short-pulse LB law) is

$$\kappa_{cc} = 1 + \frac{4/\pi}{W/\zeta} \times F(\Gamma) = 1 + \frac{4/\pi}{W/D}\bar{\zeta} \times F(\Gamma), \tag{12}$$

where ζ is the finite pulse length of electron beam in the cylindrical diode (i.e., $\zeta = r_s - r_i$ for divergent flow as illustrated in Fig. 1(b) and $\zeta = r_o - r_s$ for convergent flow), and $\bar{\zeta} = \zeta/D$ is a function of X_{CL} and Γ.

Thus, we have shown a simple method to extend the 1D short-pulse CL and LB laws to include multidimensional effect for both planar and cylindrical geometries, which can be verified by PIC simulations (see below).

D. Particle in cell simulation

PIC simulations using MAGIC2D[31] were performed to verify the analytical results for a 1D short-pulse LB law by constructing a coaxial cylindrical diode with an aspect ratio of $\Gamma = r_o/r_i$. For both divergent and convergent flows with $r_a > r_c$ and $r_a < r_c$ respectively, the cathode is grounded and the anode is given a potential of V_g. A finite emitting length W, of five times the radius of the outer shell, is created on the cathode (i.e., $W \gg 5r_o$) to confirm the limit of the 1D model. An electron beam with pulse length τ_p is injected from the cathode with an initial electron velocity of 0.1 eV to initiate electron emission. The pulse is generated using two step functions where the first step function turns on the emission at t_{rise} (rise time of the external circuit from zero to V_g) and the second one turns off the emission after $t_{rise} + \tau_p$. In the simulation, we use the over-injection method to determine the space-charge-limited condition, where the injected current is increased until a virtual cathode is formed (i.e., reflection of electrons back to the cathode start to occur).

Figures 2(a) and 2(b) illustrate the normalized 1D short-pulse LB law: $\mu_{cc} = J_{cc}(1D)/J_{LB}$ (in terms of the classical 1D long-pulse LB law) for a cylindrical diode with $\Gamma = 3$ and 10 as a function of the normalized transit time X_{CL}. The normal-

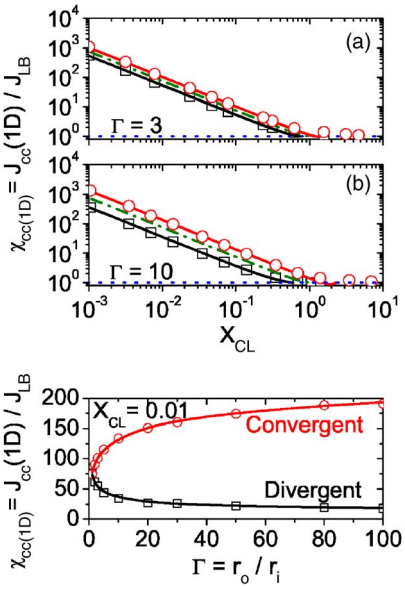

FIG. 2. (Color online) The normalized 1D short-pulse LB law $\chi_{cc(1D)}=J_{cc}(1D)/J_{LB}$ of a coaxial cylindrical diode (a) with aspect ratio $\Gamma=3$ and (b) $\Gamma=10$, for both convergent (top) and divergent (bottom) electron flows as a function of normalized transit time X_{CL}. (c) The normalized 1D short-pulse LB law $\chi_{cc(1D)}=J_{cc}(1D)/J_{LB}$ at $X_{CL}=0.01$ as a function of aspect ratio from $\Gamma=1.1$ to $\Gamma=100$. Symbols represent PIC simulation (MAGIC) results (circle: convergent and squares: divergent). The solid lines are the analytical results. The dashed-dotted lines are the normalized 1D short-pulse CL law (at $\Gamma\approx 1$) $\mu_{cp(1D)}=J_{cp}(1D)/J_{CL}$ for a planar diode with gap spacing $D=r_o-r_i$.

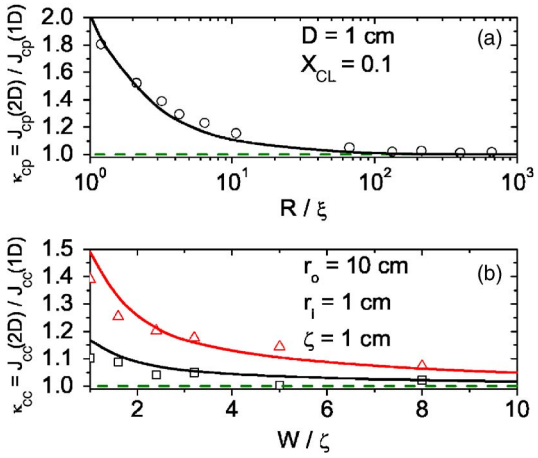

FIG. 3. (Color online) (a) The normalized 2D short pulse CL law $\kappa_{cp}=J_{cp}(2D)/J_{cp}(1D)$ for a circular emission patch at $X_{CL}=0.1$ as a function of various $R/\xi=1$ to 1000. (b) The normalized 2D short pulse LB law $\kappa_{cc}=J_{cc}(2D)/J_{cc}(1D)$ of a coaxial cylindrical diode at $\Gamma=10$ as a function of the normalized cathode width W/ζ for convergent (top) and divergent (bottom) electron flows. Symbols represent MAGIC2D planar simulations (circles) and cylindrical simulations (triangles: convergent and squares: divergent) results. Solid lines are the 2D analytical results.

ized 1D short-pulse CL law (planar limit) is also plotted for comparison (the dash-dotted lines). Figures 2(a) and 2(b) show good agreement between the PIC simulation results and the 1D analytical short-pulse LB law shown previously over a wide range of X_{CL}, and they recover to the long-pulse limits at $X_{CL}=1$. Various inner shell radii r_i (i.e., $r_i=1$ cm for $\Gamma=3$ and $r_i=0.1$ cm for $\Gamma=10$) had been used to ensure that the 1D analytical results agree well with the MAGIC simulations for different coaxial cylindrical diode dimensions. It is interesting to note that the enhancement for divergent flow is always smaller than that of convergent flow, similar to the reported long-pulse results.[26] As Γ increases from 3 to 10, the difference in the enhancement due to the finite pulse length X_{CL} between the convergent and divergent flows can be more than one order of magnitude at small X_{CL}. As an example, at $\Gamma=3$ and $X_{CL}=0.01$, the enhancement is $\mu_{cc}=6.2$ and 131 for divergent and convergent flows, respectively.

In Fig. 2(c), we show the 1D short-pulse LB law from $\Gamma=1.1$ to 100 at $X_{CL}=0.01$. From Fig. 2(c), we observe that both convergent and divergent flows are nearly identical at $\Gamma=1.1$, which recovers to the 1D short-pulse CL law as expected. The analytical solutions (solid lines) are accurate with an error of 6% for the range of $1.1\leqslant\Gamma\leqslant 100$ as compared to PIC simulation. For a convergent (or divergent) flow, the enhancement of the 1D short-pulse LB law increases (or decreases) rapidly and saturates at large Γ. At $\Gamma=100$, we have $\chi_{cc}=18$ and 191 for divergent and convergent flows respectively and the variation at larger $\Gamma>100$ is negligible.

In additional to the verification of the 1D short-pulse LB law, we also verify our 2D CL and LB laws as formulated in the previous section using PIC simulation. Note that the 1D short-pulse CL law has been verified in a previous article.[30] To verify the 2D short-pulse CL law as shown in Eq. (11), we have also used the 2D PIC simulation code MAGIC2D.[31] Consider a planar gap with gap distance $D=1$ cm and gap voltage $V_g=1$ kV, and the electron emission is limited to a finite circular area of radius R on the cathode (0.08 cm$\leqslant R\leqslant$5 cm). The short electron beamlet is also created by two step functions restrict the electron emission time to τ_p similar to the previous 1D cylindrical short-pulse simulations. Uniform electron emission with (initial energy of 0.1 eV) of $\tau_p=1.59954$ ns, which is equivalent to normalized transit time $X_{CL}=0.1$ is injected into the gap. The space-charge-limited emission is determined by increasing the amount of the injected current until a virtual cathode is formed very near to the center of the cathode (i.e., electrons start to reflect back to the cathode). Figure 3(a) shows the comparison of the enhancement of the 2D short-pulse CL law $\kappa_{cp}=J_{cp}(2D)/J_{cp}(1D)$ between MAGIC2D simulation (symbols) and our planar 2D short-pulse analytical results at $X_{CL}=0.1$, which shows excellent agreement with error less than 6%.

The 2D short-pulse LB law is also verified using MAGIC2D at $\Gamma=10$ and $\zeta=0.1$ cm. As the pulse length can differ by more than an order of magnitude at the same normalized transit time X_{CL} for convergent and divergent flows, therefore, it would be more appropriate to compare both convergent and divergent cases based on the same pulse length ζ. Therefore, we choose $\zeta=0.1$ cm, $r_o=10$ cm, $r_i=1$ cm, and vary the width of the emission patch (W) in cylindrical diode. In Fig. 3(b), we confirm that our PIC simulations results (symbols) agrees well with the analytical results (solid lines) for both convergent (top) and divergent (bottom) flows. The errors for both convergent and divergent flows are all within

4% for $W/\zeta > 1.6$. Note the simulations results obtained earlier have been counter checked randomly by using another 2D PIC code: XOOPIC,[32] which show negligible difference between them.

III. SUMMARY

In summary, we have presented the 1D and 2D models of the short-pulse space-charge-limited electron emission for the planar and cylindrical geometries in the nonrelativistic regime. The 1D cylindrical short-pulse LB law and the 2D models of the 1D short-pulse CL and LB laws are derived and reported for the first time. The enhancement of the 1D short-pulse LB law is strongly dependent on the aspect ratio Γ (<10), and the enhancement is found to be higher for the convergent flow as compared to the divergent flow. The extension to 2D short-pulse models have been done based on the equivalent diode approximation from the long pulse (or steady state) formulation.[26] The 1D and 2D particle-in-cell simulations using MAGIC2D are performed to confirm the analytical short-pulse CL and LB laws. The excellent agreement implies that other geometrical enhancement factors derived under the long pulse limit[26]should also be valid for formulating other multidimensional short pulse SCL current emission models. It is important to note that multidimensional short-pulse SCL current effects studied in this article only become important with small emission area like $R \ll D$ in the 2D short-pulse CL law studied previously due to small $X_{\mathrm{CL}} < 1$. For example, the 2D effects only become important when R is comparable to ξ (for instance, $R/\xi = 1-10$ corresponds to a small $R/D = 0.0075-0.075$ at $X_{\mathrm{CL}} = 0.1$). This finding implies that the demonstration of the 2D short-pulse CL (or LB) law studied in this article may be possible by using sharp emitters (for high current emission) as the photocathode operating at the space-charge limit under high power laser excitation.

ACKNOWLEDGMENTS

This work was supported by the Agency for Science, Technology and Research of Singapore (Reference No. 042 101 0080). Two of the authors (W.S.K. and L.K.A.) would like to acknowledge the support of computing resources by BIRC in Nanyang Technological University, Singapore.

[1] D. H. Dowell, S. Joly, A. P. de Brion, and G. Haouat, Phys. Plasmas **4**, 3369 (1997).
[2] D. Sertore, S. Schreiber, K. Floettmann, F. Stephan, K. Zapfe, and P. Michelato, Nucl. Instrum. Methods Phys. Res. A **445**, 422 (2000).
[3] T. Siggins, C. Sinclair, C. Bohn, D. Bullard, D. Douglas, A. Grippo, J. Gubeli, G. A. Krafft, and B. Yunn, Nucl. Instrum. Methods Phys. Res. A **475**, 549 (2001).
[4] D. C. Nguyen, P. L. Colestock, S. S. Kurennoy, D. E. Rees, A. H. Regan, S. Russell, D. L. Schrage, R. L. Wood, L. M. Young, T. Schultheiss *et al.*, Nucl. Instrum. Methods Phys. Res. A **528**, 71 (2004).
[5] J. Smedley, T. Rao, and Q. Zhao, J. Appl. Phys. **98**, 043111 (2005).
[6] I. Boscolo and P. Michelato, Nucl. Instrum. Methods Phys. Res. A **445**, 389 (2000).
[7] K. Zhao, J. K. Hao, Y. X. Tang, L. F. Wang, B. C. Zhang, and J. E. Chen, Nucl. Instrum. Methods Phys. Res. A **445**, 394 (2000).
[8] K. L. Jensen, D. W. Feldman, and P. G. O'Shea, Appl. Phys. Lett. **85**, 5448 (2004).
[9] J. W. Lewellen and C. A. Brau, Nucl. Instrum. Methods Phys. Res. A **507**, 323 (2003).
[10] B. Faatz, A. A. Fateev, K. Flottmann, D. Nolle, P. Piot, E. L. Saldin, H. Schlarb, E. A. Schneidmiller, S. Schreiber, D. Sertore *et al.*, Nucl. Instrum. Methods Phys. Res. A **507**, 350 (2003).
[11] M. D. Perry, D. Pennington, B. C. Stuart, G. Tietbohl, J. A. Britten, C. Brown, S. Herman, B. Golick, M. Kartz, J. Miller *et al.*, Opt. Lett. **24**, 160 (1999).
[12] C. D. Child, Phys. Rev. (Series I) **32**, 492 (1911).
[13] I. Langmuir, Phys. Rev. **2**, 450 (1913).
[14] I. Langmuir and K. B. Blodgett, Phys. Rev. **22**, 347 (1923).
[15] I. Langmuir and K. T. Compton, Rev. Mod. Phys. **3**, 191 (1931).
[16] G. Jaffe, Phys. Rev. **65**, 91 (1944).
[17] S. Y. Liu and R. A. Dougal, J. Appl. Phys. **78**, 5919 (1995).
[18] P. V. Akimov, H. Schamel, H. Kolinsky, A. Y. Ender, and V. I. Kuznetsov, Phys. Plasmas **8**, 3788 (2001).
[19] H. R. Jory and A. W. Trivelpiece, J. Appl. Phys. **61**, 2160 (1969).
[20] Y. Y. Lau, D. Chernin, D. G. Colombant, and P.-T. Ho, Phys. Rev. Lett. **66**, 1446 (1991).
[21] L. K. Ang, T. J. T. Kwan, and Y. Y. Lau, Phys. Rev. Lett. **91**, 208303 (2003).
[22] L. K. Ang, W. S. Koh, Y. Y. Lau, and T. J. T. Kwan, Phys. Plasmas **13**, 056701 (2006).
[23] J. W. Luginsland, Y. Y. Lau, and R. M. Gilgenbach, Phys. Rev. Lett. **77**, 4668 (1996).
[24] J. W. Luginsland, Y. Y. Lau, and R. M. Gilgenbach, Phys. Rev. Lett. **78**, 2680 (1997).
[25] Y. Y. Lau, Phys. Rev. Lett. **87**, 278301 (2001).
[26] W. S. Koh, L. K. Ang, and T. J. T. Kwan, Phys. Plasmas **12**, 053107 (2005).
[27] K. G. Kostov and J. J. Barroso, Phys. Plasmas **9**, 1039 (2002).
[28] J. P. Girardeau-Montaut and C. Girardeau-Montaut, J. Appl. Phys. **65**, 2889 (1989).
[29] G. Travish, D. Giove, P. Michelato, C. Pagani, P. Pierini, L. Serafini, and D. Sertore, Proceedings of the Sixth European Particle Accelerator Conference (EPAC'98), 1998, Vol. D05, p. 1133.
[30] Á. Valfells, D. Feldman, M. Virgo, P. G. O'Shea, and Y. Y. Lau, Phys. Plasmas **9**, 2377 (2002).
[31] B. Goplen, L. Ludeking, D. Smithe, and G. Warren, Comput. Phys. Commun. **87**, 54 (1995).
[32] J. P. Verboncoeur, A. B. Langdon, and N. T. Gladd, Comput. Phys. Commun. **87**, 199 (1995).